Interdigitated Array Microelectrodes for the Determination of Enzyme Activities*

Ulla Wollenberger, Manfred Paeschke and Rainer Hintsche

Fraunhofer-Institute for Silicon Technology, Dillenbunger Str. 53, 14199 Berlin, Germany

An array of closely spaced interdigitated microelectrodes was applied to the sensitive detection of reversible redox couples. The measurement is based on the redox cyclization between the adjacent microband electrodes of the interdigitated array (IDA), when both the respective oxidation and reduction potential are applied at the electrode pairs. The multiple oxidation and reduction result in an increased generation of current. The steady-state current of mediators, such as phenazine methosulfate, hexacyanoferrate(II), pyrocatechol, benzoquinone and *p*-aminophenol, was amplified by a factor of 10–20 compared with the current of single electrodes. The high collection efficiency enabled this signal amplification rate to be obtained. The detection limit for *p*-aminophenol was 100 nmol l^{-1}. The IDA sensor was applied to the determination of alkaline phosphatase and ß-galactosidase activity by detecting enzymatically generated *p*-aminophenol.

Keywords: *Microelectrode; interdigitated array; redox recycling; enzyme activity*

Introduction

The microfabrication of electrodes in silicon technology opens new dimensions in structuring transducer elements for micro-size sensor probes. Microelectrodes are attracting interest because they exhibit a fast establishment of steady-state or quasi steady-state currents, diffusion-controlled currents, low charging currents, and reduced solution resistance effects.[1] Hence, miniaturization of electrodes has led to new fields of analytical application, such as rapid voltammetric measurement in low conducting media and very small sample volumes, *in vivo* assays, electrochemical diodes and ion-selective field effect transistor (ISFET) devices.[2] Furthermore, their potential for microsystem integration makes these electrodes particularly attractive.

With the arrangement of more than one microelectrode in an array, new functions can be achieved. Planar interdigitated electrode arrays with closely spaced microband electrodes have been used for conductimetric and voltammetric techniques.[3] A number of papers have been published describing theoretical and experimental studies of diffusion in microband electrodes.[1,4–10] The mass transport of electroactive species is non-linear. As the gap between the microbands is less than a few micrometres, which is of the same order as the diffusion layer thickness, the layers overlap. This effect makes them suitable for the study of charge-transfer kinetics and electrochemical characterization of redox polymers.[1,4–8] For analytical purposes it is particularly important that the product of an electrochemical reaction can be detected at the adjacent electrode.

The situation is analogous to experiments with rotating ring–disc electrodes, where the intermediate generated on the disc (generator) electrode is subsequently detected at the ring (collector) electrode with the exception that diffusion, rather than convection, is the primary means of mass transport.[11] When the potential difference between two microband electrodes is adjusted sufficiently, electrolytic steady-state concentration gradients of oxidized and reduced redox molecules are established in the inter-electrode gap. In contrast to rotating ring–disc electrodes, the molecule converted at the collector electrode diffuses back to the generator electrode where it is again electrochemically transformed. Hence, multiple oxidation and reduction can be observed (Fig. 1). This redox recycling creates both a steady-state response and high (amplified) current. Theoretical considerations demonstrate that the limiting current is not only dependent on the concentration and diffusion coefficient of the redox species, but is also related to the lateral dimension of the gap.[2,9,12] By reducing the spacing to below 5 μm, the

* Presented at Euroanalysis VIII, Edinburgh, Scotland, UK, September 5–11, 1993.

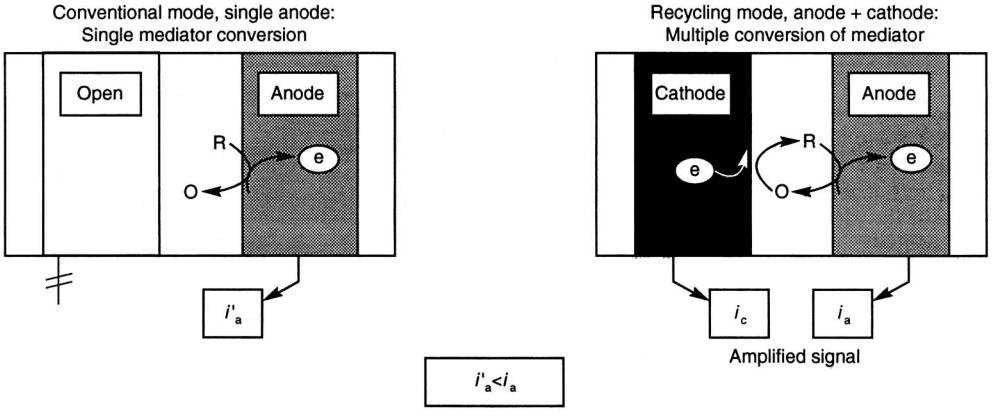

Fig. 1 Schematic diagram of the redox recycling of oxidized (O) and reduced (R) redox species with closely spaced microelectrodes. i_a and i_c represent anodic and cathodic currents, respectively; i'_a is the unamplified current response of the single anode.

collection efficiency approaches unity. A further reduction of the lateral structures to nanometre dimensions will only affect the amplification factor, which could increase considerably.

Bard and co-workers[1] defined the collection efficiency as the ratio of the currents at the generator and collector electrodes. The ratio between the steady-state currents of the generator electrode with and without connecting the collector electrode is the amplification factor. Recently, the potential of interdigitated arrays (IDAs) for the enhancement of analytical performance of detectors with respect to selectivity[13,14] and sensitivity[12,13] has been demonstrated.

p-Aminophenol can be reversibly oxidized and reduced, whereas various aminophenylated compounds exhibit an irreversible electrochemical behaviour. Therefore, assays have been proposed for the determination of alkaline phosphatase[15,16] and α-amylase[17] based on the measurement of the current produced by the electrochemical oxidation of enzymically formed *p*-aminophenol. Furthermore, the utility of *p*-aminophenyl phosphate in enzyme immunoassays has been demonstrated.[18–21]

Because the electrochemical behaviour of *p*-aminophenol is advantageous for voltammetric detection at twin electrodes, highly sensitive detection at IDAs in the redox recycling mode can be expected. This has been reported recently by Niwa *et al.*[22] for an electrochemical enzyme immunoassay.

This paper describes the application of arrays of sub-micrometre spaced IDAs to the sensitive measurement of redox mediators based on multiple electrochemical recycling. Simultaneously, reference measurements have been performed with other electrodes at the sensor chip. In addition, the measuring principle has been used for the determination of hydrolytic enzymes.

Experimental

Reagents

p-Aminophenol, hydroquinone, benzoquinone, pyrocatechol, naphthol and potassium hexacyanoferrate(II) were obtained from Aldrich (Steinheim, Germany). *P*-Aminophenyl ß-D-galactopyranoside (*p*-APG) was obtained from USB. (Bad Homburg, Germany). *p*-Aminophenyl phosphate was synthesized from *p*-nitrophenyl phosphate (Fluka, Buchs, Switzerland) according to a literature method.[23] Alkaline phosphatase (EC 3.1.3.1) from calf intestine was purchased from Boehringer Mannheim (Mannheim, Germany) and ß-galactosidase (EC 3.2.1.23) from *Escherichia coli* was a product of Sigma (St. Louis, MO, USA).

All other reagents were of analytical-reagent grade and all solutions were prepared in doubly distilled water. The mediator and enzyme substrate solutions were kept in dark containers.

Electrode

The IDA electrodes and connectors were fabricated by standardized silicon technology. Titanium (20 nm thick) and platinum (200 nm thick) were evaporated onto a thermally oxidized silicon wafer and structured using a lift-off technique. A schematic diagram of the electrode pattern and a scanning electron micrograph of the sensing area are shown in Fig. 2. Four pairs of microbands were arranged on one chip. Each finger electrode is 900 μm long and 3.2 μm wide. The gaps between the finger electrodes are 0.8 μm. The chips (8 × 8 mm^2) were encapsulated by a 400 nm thick plasma-enhanced chemical vapour deposition (PECVD) SiO_2 layer, excluding the 2.8 × 0.9 mm^2 electrode area and the connecting pads.[24] The separated IDAs were electrically tested for 'shorts' between the band electrodes. Only chips with a resistance between interdigitated electrodes of more than 20 MΩ in the dry state were used. The chip sensor was electrically connected by means of gold wires bonded to the pads. These bonds were covered with silicone rubber resin (Dow Corning, Midland, MI, USA).

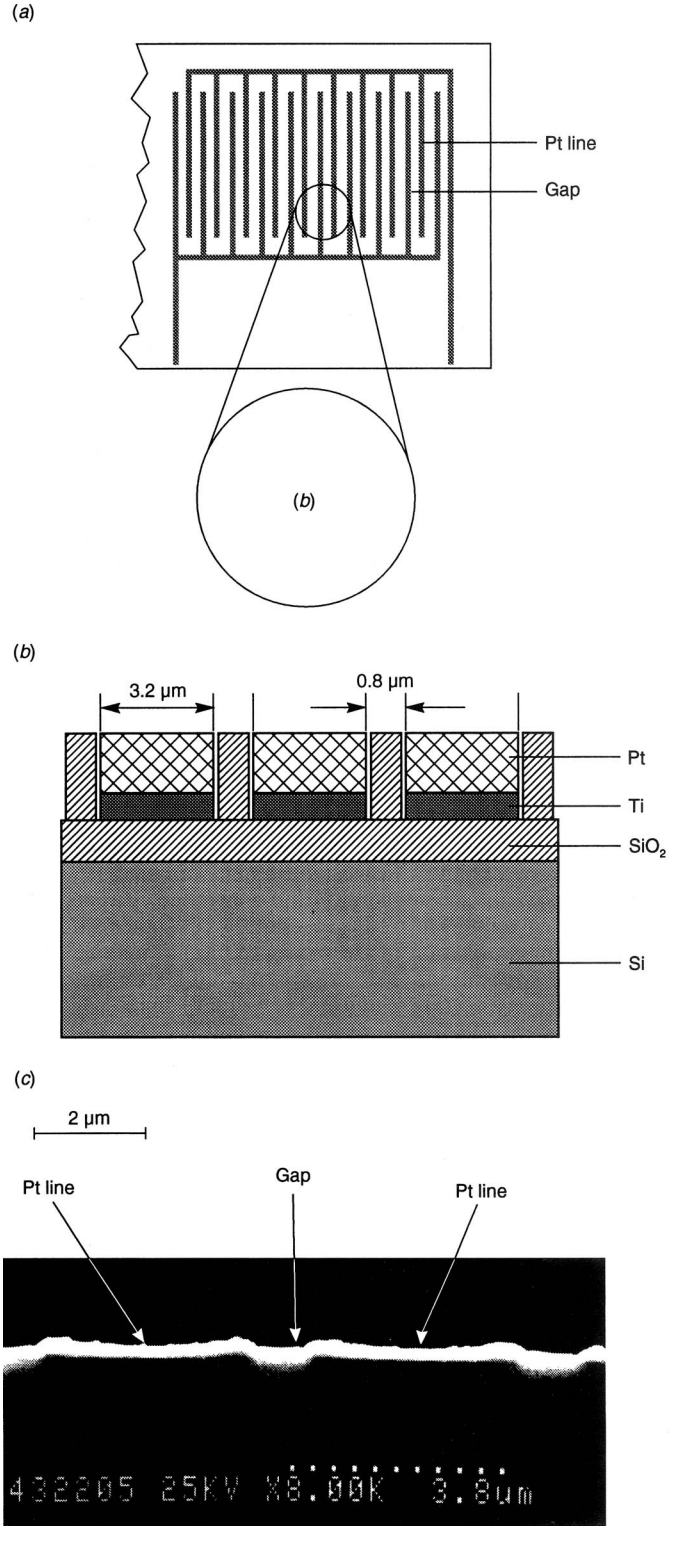

Fig. 2 (*a*) Illustration of the Pt-band pattern of the interdigitated electrode array. (*b*) Schematic cross-sectional view of the microband electrodes. (*c*) Scanning electron micrograph of the microband electrodes.

Apparatus

Electrochemical measurements were carried out in 10 ml of solution using an Ag–AgCl reference electrode (Bioanalytical Systems, West Lafayette, IN, USA). A custom-made multipotentiostat was used to control the potential of the electrodes independently. The current response of the individual electrodes was separately preamplified after current-to-voltage conversion and sent to a data acquisition board.

Cyclic voltammograms were obtained with an Auto-Lab PSTAT 10 electrochemical analyser (ECO Chemie, Utrecht, The Netherlands). All measurements were performed at 25 °C.

Buffers

The following buffer solutions were used. Buffer solution A: 0.066 mol l^{-1} potassium phosphate–sodium phosphate and 0.1 mol l^{-1} KCl, pH 7.0. Buffer solution B: 0.1 mol tris(hydroxymethyl)aminomethane(Tris), 0.001 mol l^{-1} $MgCl_2$ and 0.01 mol l^{-1} diethanolamine adjusted to pH 9.6 with HCl. Buffer solution C: 0.1 mol l^{-1} Tris, 0.01 mol l^{-1} NaCl adjusted to pH 7.3 with HCl.

Buffer solution A was used throughout the basic investigations of mediator recycling. Buffer solution B was used for the experiments with alkaline phosphatase and buffer solution C for ß-galactosidase measurements.

Results and Discussion

The principle of the sensitive detection of mediators was demonstrated for measurement of *p*-aminophenol with IDAs. In order to define the optimum potentials for oxidation and reduction of the mediator, cyclic and hydrodynamic voltammograms were recorded. In a further experiment, the potential of one electrode, the generator electrode, that detects *p*-aminophenol was changed stepwise in the positive direction, while the potential of the adjacent electrode, the collector electrode, was maintained at −50 mV such that the quinoneimine generated was reoxidized to aminophenol. A third microband electrode on the IDA chip was investigated simultaneously, but without an (interdigitated) collector electrode. An increase in both anodic and cathodic limiting currents is observed, reaching a maximum value at a generator potential of about 300 mV (Fig. 3). The magnitude of the limiting currents (anodic and cathodic) is much larger than the current of the 'single' anode. This is clearly a manifestation of the redox cycling between the generator electrode (when a sufficient overpotential is applied) and the collector electrode, and demonstrates that the collector electrode is an additional source of *p*-aminophenol to the generator electrode. The ratio of cathodic to anodic current, *i.e.*, the collection efficiency,[4] is 0.92, *i.e.*, 92% of the oxidation product formed at the anodic current generator is collected at the adjacent cathode, where *p*-aminophenol is produced, which undergoes a cyclic redox reaction again. The very high magnitude of the collection efficiency suggests that the distance between the adjacent electrodes is of the same order as the diffusion layer thickness and that with the close spacing of the anode and cathode in the IDA with a large number of alternating microbands, radial diffusion dominates transport into the bulk solution.

Fig. 4 shows the dependence of the anodic and cathodic steady-state currents at one pair of IDA electrodes on *p*-aminophenol concentration when the anode potential was fixed at +250 mV and the cathode potential was −50 mV. The addition of 10 µmol l^{-1} *p*-aminophenol results in an anodic current of 160 nA within 1 s. A similar response is registered simultaneously at the cathode. Again, *p*-aminophenol diffuses

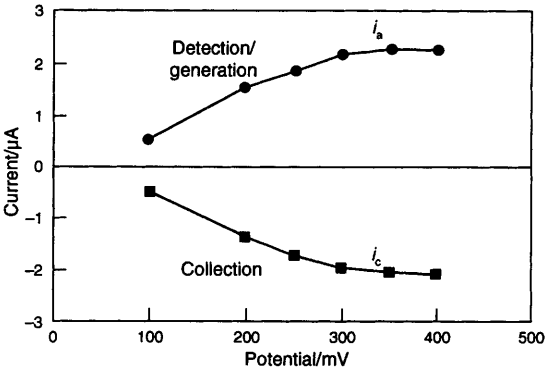

Fig. 3 Hydrodynamic voltammogram for 200 µmol l^{-1} of *p*-aminophenol obtained with a single microband electrode held at −50 mV and the adjacent electrode potential varied between 100 and 400 mV *versus* Ag–AgCl–1 mol l^{-1} KCl. The background solution was buffer solution A. i_a = anodic current; i_c = cathodic current.

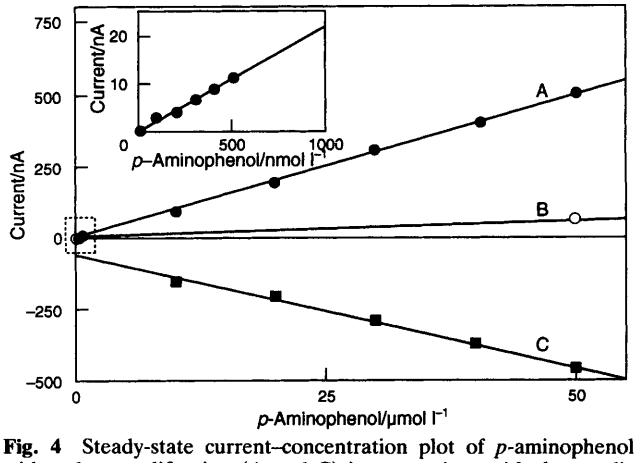

Fig. 4 Steady-state current–concentration plot of *p*-aminophenol with redox amplification (A and C) in comparison with the anodic response with an open cathode (B) and illustration of the sensitivity (inset). Interdigitated electrodes were polarized at +250 and −50 mV *versus* Ag–AgCl–1 mol l^{-1} KCl.

Table 1 Parameters of mediators: i = current; i_a = anodic current; i_c = cathodic current; and i' = current measured with the generator electrode without connecting the collector

Mediator	Anode potential/mV	Cathode potential/mV	Sensitivity*/ nA l µmol^{-1}	Amplification Factor* (i/i')	Collection efficiency* (i_c/i_a)
$Fe(CN)_6^{4-}$	350	−120	2.8	8	0.98
Pyrocatechol	600	−200	7.2	9	0.92
p-Benzoquinone	400	−75	5.7	14	0.94
p-Aminophenol	250	−50	16.4	12	0.92
Phenazine methosulfate	0	−200	18.6	12	0.95

* Average values.

to the anode where it is detected, while the oxidation product is collected at the adjacent cathode. Here, it is converted back to its initial state.

In comparison, the single anode shows a poor response at this low substrate concentration. A single cathode shows no response at all, which is to be expected as the distance to the generator/collector IDA is about 1 mm.

The amperometric response is enhanced by a factor of 10–15 by the electrochemical cycling. Hence, the detection limit could be improved to 100 nmol l^{-1} with reasonable reproducibility.

A number of mediators were similarly investigated. Table 1 summarizes the results for sensitivity, amplification factor and collection efficiency. As can be seen, collection efficiencies of about 0.9 were achieved for all the reversible redox couples studied.

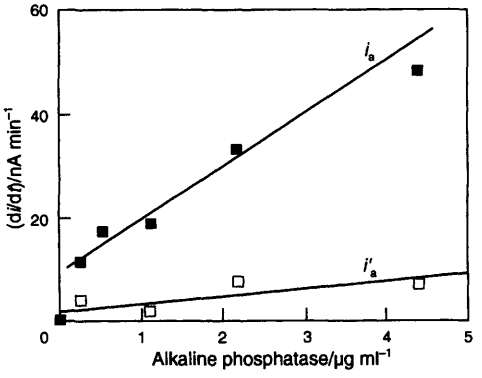

Fig. 5 Calibration graph of alkaline phosphatase assay. The incubation medium was buffer solution B and 2 mmol l^{-1} of *p*-aminophenyl phosphate; the IDA was as in Fig. 4. i_a = anodic current; i'_a = unamplified current response of the single anode.

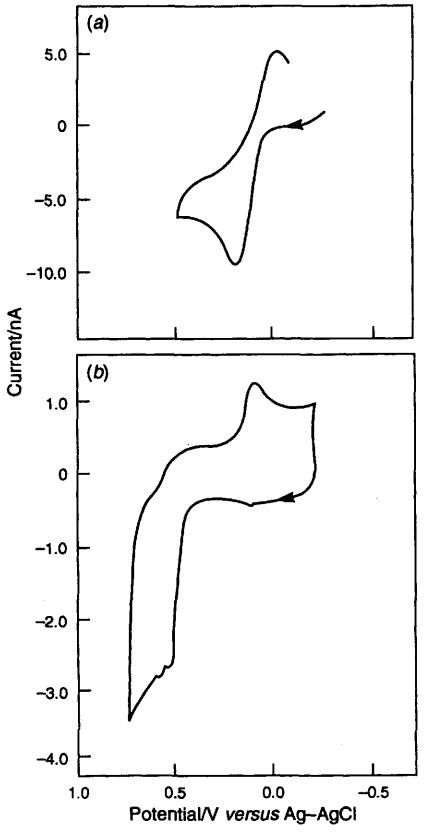

Fig. 6 D.c. cyclic voltammograms of (*a*) *p*-aminophenol and (*b*) *p*-APG recorded in buffer solution A at Pt electrodes. The sweep rate was 100 mV s^{-1} between −300 and +700 mV *versus* Ag–AgCl–1.0 mol l^{-1} KCl.

This compares well with theoretical predictions and experimental studies of IDAs with a large number of alternating microband electrodes having a width of 2 μm and a gap of 1 μm.[1,12] The amplification factors of 10–15 are of the same order of magnitude as recently published values for dopamine.[14] The short average diffusion length and the large number of alternating electrodes used are necessary for effective current amplification by redox recycling.

The limiting currents are essentially stable over a period of more than 1 h. The application of this detection principle to enzyme assays is discussed in the next section.

Enzyme Assays

Alkaline phosphatase and ß-galactosidase are the most frequently used enzyme labels in enzyme immunoassays. Therefore, the IDA described here was applied to the measurement of alkaline phosphatase [eqn. (1)] and ß-galactosidase [eqn. (2)] activity by quantifying the rate of *p*-aminophenol formation during hydrolysis

Alkaline phosphatase:

$$p\text{-aminophenyl phosphate} \rightarrow p\text{-aminophenol} + \text{phosphate} \quad (1)$$

ß-*Galactosidase:*

$$p\text{-APG} \rightarrow p\text{-aminophenol} + \text{ß-D-galactopyranoside} \quad (2)$$

In the alkaline phosphatase assay with the proposed redox recycling measuring principle at IDAs, *p*-aminophenyl phosphate was used as the substrate. This substrate has advantages over other phenolic substrates. It is enzymically dephosphorylated faster than nitrophenyl phosphate and phenyl phosphate; *p*-aminophenol is oxidized at lower overvoltages than unsubstituted phenol, and does not cause electrode fouling on electro-oxidation.

Furthermore, the difference in the oxidation peak potentials of *p*-aminophenol and its phosphate is >300 mV. Hence, *p*-aminophenol could be easily detected by electrochemical oxidation without interference from the substrate. For the measurement procedure used here, the excellent electrochemical reversibility of *p*-aminophenol is particularly important.

When the hydrolysis was performed under the optimum conditions for alkaline phosphatase, *i.e.*, in buffer solution B, in the presence of excess of *p*-aminophenyl phosphate, a non-

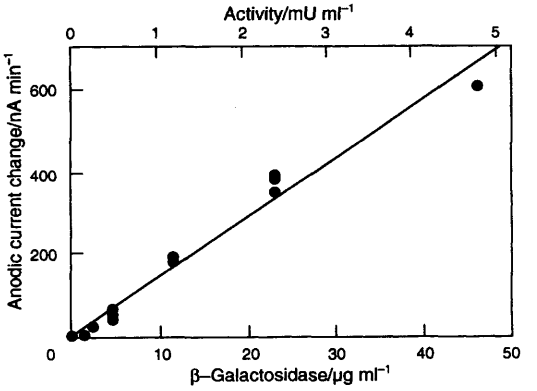

Fig. 7 Dependence of rate of current increase on ß-galactosidase concentration. The conditions were: 5 mmol l^{-1} of *p*-APG in buffer solution C; the IDA was as in Fig. 4.

linear anodic current increase could only be obtained. No recycling effect was observed.

The study of the recycling at various pH values revealed its dependence on pH. Maximum amplification (redox recycling) occurred at pH 6.8–7.6. At higher pH values, the amplification rate decreased markedly. Above pH 9.0, no amplification was observed. The anodic current with and without potentiostating the cathode was the same. No cathodic current response was detected. The lack of reversibility might be due to the generation of polymeric products and to the instability of *p*-aminophenol in alkaline solution.[20,25] The *para*-substitution promotes oxidation. Therefore, *p*-aminophenol is very sensitive to oxygen and (ultraviolet) light. Its stability is much higher at pH 8.0 and only a very small decay was observed at neutral pH. However, for the assay of alkaline phosphatase, a low pH is unfavourable. Therefore, the enzyme was incubated externally in a dark container, which was filled with 1 ml of buffer solution B, with 2 mmol l^{-1} of *p*-aminophenyl phosphate [*i.e.*, about 30 times higher than the value of the apparent Michaelis–Menten constant (K_m')].[16] After 2 and 5 min, 100 μl of the incubation solution were transferred into the measuring cell containing 10 ml of buffer solution A. The resulting current increase represents the formation of *p*-aminophenol in the external container. From a comparison of the response, and from a calibration for *p*-aminophenol, the enzyme activity of the sample was calculated (Fig. 5).

For the determination of ß-galactosidase, *p*-APG was chosen as the substrate. Cyclic voltammograms were recorded at Pt electrodes to characterize the substrate–product couple (Fig. 6). The oxidation waves of *p*-aminophenol and *p*-APG exhibit peak potentials at +200 and +550 mV, respectively. Therefore, the product (*p*-aminophenol) of the enzymic hydrolysis could easily be detected without interference from the substrate (*p*-APG). The reduction peak represents the appearance of the quinoneimine compound during the oxidation of *p*-APG. This peak is not observed when the cyclic voltammetric experiment is performed between −200 and +300 mV. The second scan of *p*-APG exhibits an increased oxidation peak at the same potential as *p*-aminophenol. This indicates that, during the electro-oxidation of *p*-APG, *p*-aminophenol is liberated.

The weak oxidation wave observed at a potential of about +200 mV suggests that *p*-aminophenol is present as an impurity in the *p*-APG preparation. This impurity causes a blank signal of 220 nA when the 5 mmol l^{-1} of enzyme substrate are injected into the measuring cell. Because the rate of current change is monitored, the blank does not contribute to the current change after oxidation of the enzyme. Moreover, the blank background current is stable for more than 2 h, indicating that *p*-APG is stable at pH 7.3. Although *p*-aminophenol is unstable in alkaline solution, this behaviour was not observed at the neutral pH used. After introduction of the calibration solution into the measuring cell, a constant steady-state current was obtained over a period of 1 h of continuous measurement. The substrate concentration of 5 mmol l^{-1} was found to be sufficiently high to maintain zero-order kinetics of the enzymic hydrolysis.

The optimum conditions were evaluated to be 5 mmol l^{-1} *p*-APG in buffer solution C.

When the current baseline of the IDA chip sensor in 10 ml of background solution (buffer solution C) with *p*-APG was stable, the system was calibrated by the addition of 100 nmol of *p*-aminophenol. One minute after the limiting current was obtained, 5 μl aliquots of the enzyme sample were added and in the initial rate of *p*-aminophenol formation was calculated from the slope of the anodic current increase (Fig. 7). The lower limit of detection (signal-to-noise ratio = 3) for ß-galactosidase was 1 mU ml^{-1}, *i.e.*, 0.5 pmol, and 0.3 mU ml^{-1}, *i.e.*, 0.1 pmol for alkaline phosphatase. The reproducibility was 8% for a sample containing 4 U ml^{-1} of alkaline phosphatase. Therefore, the proposed IDA can be used for the determination of hydrolase activities. When only one of the finger electrode pairs was potentiostated at 250 mV and the other was left open, only 10% of the sensitivity was obtained.

Future application of the sensing principle will include electrochemical immunodetection procedures in microsystems.

We thank U. Schnakenberg, T. Lisec and B. Wagner for the microfabrication of the IDAs and for many helpful discussions. We also thank W. Pilz for taking the scanning electron micrographs. U. W. and R. H. gratefully acknowledge support by the KAI e.V. (project 003500 B) and the German Minister of Research and Technology (0310090 A3).

References

1 Bard, A. J., Crayston, J. A., Kittlesen, G. P., Shea, T. V., and Wrighton, M. S., *Anal. Chem.*, 1986, **58**, 2321.
2 Aoki, K., Morita, M., Niwa, O., and Tabei, H., *J. Electroanal. Chem.*, 1988, **256**, 269.
3 Sheppard, N. F., Tucker, R. C., and Wu, C., *Anal. Chem.*, 1993, **65**, 1202.
4 Chidsey, C. E., Feldman, B. J., Lundgren, C., and Murray, R. W., *Anal. Chem.*, 1986, **58**, 601.
5 Feldman, B. J., and Murray, R. W., *Anal. Chem.*, 1986, **58**, 2844.
6 Feldman, B. J., Feldberg, S. W., and Murray, R. W., *J. Phys. Chem.*, 1987, **91**, 6558.
7 Fritsch-Faules, I., and Faulkner, L. R., *Anal. Chem.*, 1992, **64**, 1118.
8 Fritsch-Faules, I., and Faulkner, L. R., *Anal. Chem.*, 1992, **64**, 1127.
9 Nishihara, H., Dalton, F., and Murray, R. W., *Anal. Chem.*, 1991, **63**, 2955.
10 Licht, S., Cammarata, V., and Wrighton, M. S., *Science*, 1989, **243**, 1176.
11 Bard, A. J., and Faulkner, L. R., *Electrochemical Methods—Fundamentals and Applications*, Wiley, New York, 1980.
12 Niwa, O., Morita, M., and Tabei, H., *Anal. Chem.*, 1990, **62**, 447.
13 Niwa, O., Morita, M., and Tabei, H., *Electroanalysis*, 1991, **3**, 163.
14 Niwa, O., Morita, M., and Tabei, H., *Sens. Actuators, B*, 1993, **13–14**, 558.
15 Frew, J. E., Foulds, N. C., Wilshere, J. M., Forrow, N. J., and Green, M. J., *J. Electroanal. Chem.*, 1989, **266**, 309.
16 Razumas, V. J., Kulys, J. J., and Malinauskas, A. A., *Anal. Chim. Acta*, 1980, **117**, 387.
17 Batchelor, M. J., Williams, S. C., and Green, M. J., *J. Electroanal. Chem.*, 1988, **246**, 307.
18 Tang, H. T., Lunte, C. F., Halsall, H. B., and Heineman, W. R., *Anal. Chim. Acta*, 1988, **214**, 187.
19 Xu, Y., Halsall, H. B., and Heinemann, W. R., *J. Pharm. Biomed. Anal.*, 1989, **7**, 1301.
20 Kronqvist, K., Lövgren, U., Edholm, L. E., and Johansson, G., *J. Pharm. Biomed. Anal.*, 1993, **11**, 459.
21 Rosen, I., and Rishpon, J., *J. Electroanal. Chem.*, 1989, **258**, 27.
22 Niwa, O., Xu, Y., Halsall, H. B., and Heineman, W. R., *Anal. Chem.*, 1993, **65**, 559.
23 DeRiemer, L. H., and Meares, C. F., *Biochemistry*, 1981, **20**, 1606.
24 Schnakenberg, U., Benecke, W., and Lange, P., *Proceedings of Transducers '91, San Francisco, USA, 1991*, IEEE, Piscataway, NJ, 1991, p. 815.
25 Cardosi, M., Birch, S., Talbot, J., and Phillips, A., *Electroanalysis*, 1991, **3**, 169.

Paper 3/06195G
Received October 18, 1993
Accepted October 27, 1993